BOREAL ENVIRONMENT RESEARCH 14: 539–549
ISSN 1239-6095 (print) ISSN 1797-2469 (online)

Helsinki 31 August 2009

Aerosol time-of-flight mass spectrometer for measuring ultrafine aerosol particles

Totti Laitinen[1], Kari Hartonen[1], Markku Kulmala[2] and Marja-Liisa Riekkola[1]

[1)] *Department of Chemistry, Laboratory of Analytical Chemistry, P.O. Box 55, FI-00014 University of Helsinki, Finland*
[2)] *Department of Physics, Division of Atmospheric Sciences and geophysics, P.O. Box 64, FI-00014 University of Helsinki, Finland*

Received 22 Oct. 2008, accepted 7 May 2009 (Editor in charge of this article: Veli-Matti Kerminen)

Laitinen, T., Hartonen, K., Kulmala, M. & Riekkola, M.-L. 2009: Aerosol time-of-flight mass spectrometer for measuring ultrafine aerosol particles. *Boreal Env. Res.* 14: 539–549.

An aerosol mass spectrometer for ultrafine aerosol particles was constructed. The operation of the apparatus is based on the aerosol particle collection onto a metal surface over a short period. The near real-time aerosol particle collection makes possible an analysis of the particle phase compounds with short lifetimes. The collected aerosol particles are charged with a bipolar charger, size-separated by a differential mobility analyzer according to their electrical mobility and collected via electrostatic deposition on the electrically charged metal surface of a sampling valve. The collected particles are subjected to a two-step laser desorption ionization before the mass spectrometric analysis. The ionized molecules are analyzed according to their m/z ratios and detected with a micro-channel plate detector. The aerosol mass spectrometer was calibrated with different chemical compounds, and its applicability for the determination of selected organic compounds was studied. The calibration of the mass axis showed a good correlation ($R^2 = 0.9996$). Mass spectral data for ultrafine ambient aerosol particles was obtained at sub-picogram concentrations.

Introduction

Atmospheric aerosol particles and trace gases affect the quality of our lives in many ways. In polluted urban environments, they impact human health and reduce visibility (Stieb *et al*. 2002). At regional and global scales they have the potential to change climate patterns and the hydrological cycle (Lohman and Feichter 2005). Aerosol particles also influence the radiation intensity distribution that reaches the Earth's surface, thereby having a direct influence on the terrestrial carbon sink (Gu 2003).

An important feature of the atmospheric aerosol system is the formation of new atmospheric aerosol particles. Although aerosol formation takes place almost everywhere in the atmosphere (Kulmala *et al*. 2004), our knowledge of this phenomenon has serious gaps. Basic, process-level understanding of atmospheric aerosols is lacking, and our knowledge of the chemical composition of newly formed aerosol particles is deficient.

Various techniques exist for the collection and chemical analysis of aerosol particles (McMurry 2000). Traditionally, aerosol particles have been collected on filters and subjected to an extraction procedure before analysis. The sampling should be as short as possible to avoid artifact formation and rapid changes in the concentration levels of

certain compounds. In addition, some particles have lifetimes of only a few minutes or hours (Allen *et al*. 1996). Unfortunately, traditional chromatographic techniques with the mass spectrometer as a detector, as well as more sophisticated instrumental approaches (LC-MS, LC-GC-MS), are not always suitable for determination of the particle composition in the atmosphere at a particular moment (Shimmo *et al*. 2004, Anttila *et al*. 2005, Warnke *et al*. 2006, Reinnig *et al*. 2008).

The small mass of ultrafine particles presents an enormous challenge for analytical devices. The biggest issue relates to the time needed to collect a representative sample with sufficient particle mass for the analytical device to be detect. With real-time processes in particular, analysis with modern filter sampling techniques is extremely difficult. To date, the smallest particles that have been analyzed in ambient air are no more than a few nanometre in diameter (Smith *et al*. 2004b).

Aerosol mass spectrometry offers a good method to analyze atmospheric aerosols within a short time interval and without sample pretreatment (Johnston 2000, Nash *et al*. 2006). Aerosol mass spectrometer setups have been around for a decade or two. Often, chemical analysis carried out with aerosol mass spectrometers is based on single-particle analysis (Ge *et al*. 1998, Morrical *et al*. 1998, Mallina *et al*. 2000, Trimborn *et al*. 2000), where continuous aerosol flow is directed inside the mass spectrometer, while gas molecules are pumped away by differential pumping. The key link in this setup is the aerodynamic lens system developed by Liu *et al*. (1995). The system can be used to form a collimated aerosol beam without gas molecules. The main benefit of the single-particle analysis is the real-time approach. However, the method requires high vacuum pumping capacity to obtain pressures low enough for the analysis. Moreover, the analysis of ultrafine particles is difficult because the smallest particles behave like gas molecules and are pumped away during the differential pumping.

The lowest size limit of present commercial aerosol mass spectrometers is about 30 nm in vacuum aerodynamic diameter (Allan *et al*. 2006), but modified aerodynamic lens systems have been used for laboratory-generated particles down to 3 nm (Wang and McMurry 2006) and for ambient particles below 10 nm (Wang *et al*. 2006). Today, the most challenging part in the analysis of ultrafine aerosol particles is determining the organic fraction of the compounds. The inorganic part is better known. The problem is that many similar and reactive organic compounds may be present in the particles which complicates the analysis (Allan *et al*. 2006).

Some groups have constructed aerosol mass spectrometers that include a collection system (Haefliger and Zenobi 1998, Kalberer *et al*. 2002, Voisin *et al*. 2003, Emmenegger *et al*. 2004, Smith *et al*. 2004a, Öktem *et al*. 2004) The aerosol sample is collected onto a surface (e.g. filter, metal surface or wire), and then desorbed thermally or with a laser. Finally it is analyzed with a mass spectrometer. With a sample collection feature included, the sample mass in analysis can be increased and the analysis of ultrafine aerosol particles is facilitated.

Desorption and ionization of the sample are necessary steps in aerosol mass spectrometry. Various desorption and ionization techniques have been used. Ionization is most commonly done by electron ionization (EI) or laser ionization (LI) (Heard 2006, Nash *et al*. 2006). The EI method is good in the sense that it ionizes everything, but it also produces abundant fragment ions from one compound, which may be a problem where the aerosol particles contain a mixture of chemically different compounds. EI is a common method and spectral libraries have been built to assist compound identification. LI is a softer method than EI and it produces fewer fragments. The amount of fragments is dependant on laser type, flux energy and wavelength. The LI spectra are often easily interpreted and LI techniques offer better sensitivity, and they are also selective, depending on the laser wavelength and power and the sample molecules. The selectivity may also cause problems. In the analysis of ambient aerosols, for example, some molecules might not absorb the laser light at the wavelength employed are therefore are not ionized. In some specific analysis the selectivity may be beneficial. A low repeatability of the laser energy and the timing jitter can cause uncertainties in spectra in some cases.

Among the different mass analyzers exploited in aerosol mass spectrometers (Heard 2006,

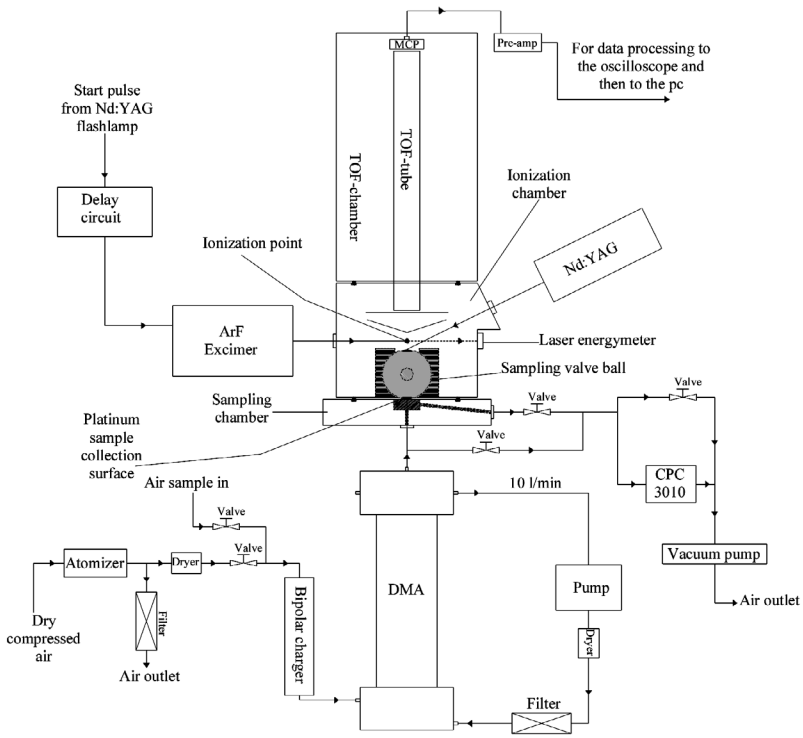

Fig. 1. Schematic of the aerosol time-of-flight mass spectrometer.

Gross 2004), the time-of-flight analyzer is the most common. The time-of-flight mass spectrometer (TOF-MS) has the capability to simultaneously and quickly analyze molecules from different chemical backgrounds over a wide range of molecular masses. Another common analyzer is the quadrupole, which is not very suitable for pulsed ionization techniques due to its slow mass scanning ability. Accordingly, the TOF-MS is commonly employed with laser desorption/ionization, and the quadrupole MS with the EI-technique.

All aerosol devices described above have been developed to provide aerosol size distribution and chemical information simultaneously in real time or near real-time. However, it is exceedingly difficult to meet these requirements with a single instrument. We have constructed an aerosol time-of-flight mass spectrometer incorporating size separation of particles, sampling, ionization and analyzing steps for the determination of the organic matter in ultrafine ambient aerosol. This paper presents a detailed description of the construction, operation and testing of our new aerosol time-of-flight mass spectrometer featuring a novel sampling valve.

Material and methods

Chemicals

Methylene blue, used for visual inspection of the collection efficiency, was purchased from Merck (Darmstadt, Germany). Test aerosol compounds, sucrose and sodium chloride (99.5%), were from Merck (Darmstadt, Germany) and 2,5-dihydroxy benzoic acid (98%) was from Merck (München, Germany). The substances used for calibration of the mass axis were pyrene (> 97%), fluoranthene (> 97%), dithranol (99%) from Fluka (Steinheim, Germany), benzoic acid from Merck (Darmstadt, Germany), 2,6-di-tert-butylpyridine (> 97%), sinapinic acid (99%) and α-cyano-4-hydroxycinnamic acid (99%) from Sigma Aldrich (Steinheim, Germany).

System description

The self-constructed aerosol time-of-flight mass spectrometer system (Fig. 1) consists of the following main parts: bipolar charger, differential mobility analyzer (DMA), sampling valve,

ionization chamber, desorption laser, ionization laser and time-of-flight mass spectrometer with vacuum chamber.

All aerosol particles are first charged with the bipolar charger. Then the particle size of interest is selected with the DMA. The size-selected charged particle flow is directed to an electrically oppositely-charged platinum collection surface, which is part of the specially designed sampling valve. This means that when a positive voltage is applied to the collection surface, negatively charged particles are attracted towards the surface. The sample flow towards the sampling surface is controlled by HEPA-filtered pressurized air and a pre-vacuum pump (Edwards RV5, England). The aerosol particles are counted with a condensation particle counter (CPC) (CPC 3010, TSI, MN, USA) before and after the collection. The collected sample is introduced to the high vacuum of the mass spectrometer (MS) by rotating the sampling valve. The high vacuum, $\sim 10^{-7}$–10^{-8} torr, in the MS side is achieved by combination of the pre-vacuum pump (Pfeiffer vacuum, rotary vane vacuum pump DUO 2.5, Asslar, Germany) and the Pfeiffer high vacuum pump (Pfeiffer vacuum, turbo molecular drag pump TMH 071 P, Asslar, Germany). The pressure is measured with a full range vacuum gauge (Pfeiffer vacuum, Compact full range vacuum gauge PKR 251, Asslar, Germany).

The sample is introduced from the atmospheric-pressure to the high-vacuum side and after the vacuum is recovered (normally 30 to 60 seconds), desorption is performed. The sample is desorbed with a single laser shot from the IR-laser (New wave research, Polaris II, Fremont, USA), which operates at the 1064 nm wavelength. The sample desorption produces a gaseous plume of mostly neutral molecules in the vacuum, which will expand rapidly. Immediately after the desorption pulse, the sample molecules in the plume are ionized with one laser shot from an ArF excimer laser (Neweks, excimer laser PSX-100, Tallinn, Estonia), operating at the wavelength of 193 nm. The lasers are placed so that the desorption laser hits the sample surface at the angle of 45° and the ionization laser is perpendicular to the TOF tube. The delay between the lasers is generated by a self-made delay circuit and usually is set to about 60 μs.

The ions produced are directed to a micro channel plate detector (MCP) (Hamamatsu, F4655-12, Japan) through a linear flight tube by a two-step ion acceleration. The acceleration lens system and the detector voltages (voltages controlled by HP 2.5, Applied kilovolts, Worthing, UK) are set to be on all the time. Data acquisition with the oscilloscope (Tektronix 2024, USA) starts exactly when the ionization laser fires. Before the data acquisition, the signal is amplified with a pre-amplifier (Philips, signal pre-amplifier B-50, UK).

Before a new sample is introduced into the system, the collection surface is cleaned by shooting a few high-power shots from the desorption laser into the collection surface. This is done to prevent contamination from a previous sample. A blank sample is run before each new sample. This can be done in two ways: by running the collection for 10 minutes without collection voltages on the collection surface or running the system with voltages off on the DMA. The blank sample is introduced to the high vacuum and analyzed to discover any contamination in the collection surface. If the blank sample is clean the next sample can be introduced into the system. In an early system we added pure nitrogen sheath flow to the collection surface to keep it clean. This measure was abandoned, however, since it did not improve the results, and the operation is much simpler and faster without it.

The sampling valve

The design of the novel sampling valve (Fig. 2) is based on Hartonen *et al*. (2006). A hollow polyacetal turning shaft is connected to a stainless steel ball 40 mm in diameter. Two high-voltage feedthroughs are secured inside the shaft with Viton O-rings. The feedthroughs are connected to the polished platinum collection surfaces, 4 mm in diameter, at either side of the ball valve and sealed with Viton O-rings (stainless steel was tested as collection surface but abandoned because it oxidizes too rapidly). The valve is easily assembled and taken apart since all parts are connected by bolt-on junctions. The two sampling surfaces enable simultaneous sample collection and analysis.

The collection properties of the sampling valve were examined visually with use of methylene blue particles (10 mg l^{-1} solution) produced with an atomizer (Topas AMT 220, Dresden, Germany). This test was strictly qualitative, with an unknown sensitivity and it was done only to verify the success of the particle collection. After the collection of particles for 20 minutes at the flow rate of 1 l min^{-1} at the collection voltage of 1.25 kV, all surfaces were wiped with a white tissue wetted with methanol to see whether dye particles were present on any other surfaces of the collection chamber than the sample collection surface.

The collection losses were calculated by measuring the transmission efficiency of the aerosol flow (1 l min^{-1}) through the sampling chamber without collection voltage on the collection surface and by comparing that transmission efficiency to the transmission efficiency without the valve in the system. The particles were counted with the CPC (TSI 3010) and particle sizes were varied between 8 and 100 nm. The test was performed by generating aerosol particles with the atomizer from a sucrose solution (10 mg l^{-1}).

The valve collection efficiency, Eff. (%), was measured with the setup depicted in Fig. 1. The aerosol particles were generated with the atomizer using sodium chloride solution (10 mg l^{-1}) as a test liquid. The particles were size-segregated with the DMA, and those deposited on the valve were counted with the CPC. The amount of particles entering the CPC before and after the voltage application was calculated for the collection efficiencies. Particle size was varied between 6 and 70 nm and collection voltage between 1.25 and 2.99 kV.

The particle desorption from the sampling surface was investigated visually with a scanning electron microscope (SEM) (Hitachi S-4800, Japan). The reference substrate for the sampling surface was of stainless steel and polished in the same way as the valve sampling surface. The thickness of the reference plate was similar to that of the sampling valve surface, 5 mm. With a microsyringe, 2 μl of 10 ppm 2,5-dihydroxybenzoic acid (DHB) solution in methanol was applied to the reference surface. After the solvent was evaporated, the DHB was vaporized and desorbed with a single 5-ns IR laser pulse (energy 40 mJ/pulse at 1064 nm, beam spot size 4 mm).

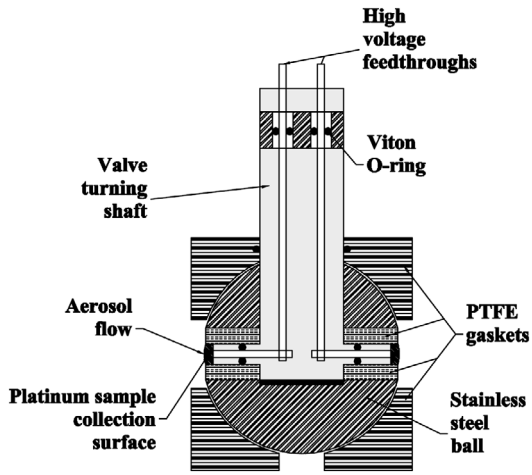

Fig. 2. Detailed construction of the sampling valve.

System calibration

The aerosol mass spectrometer was calibrated with benzoic acid, DHB, pyrene, α-cyano-4-hydroxycinnamic acid (ACCA), 2,6-di-tert-butylpyridin, fluoranthene, dithranol and sinapinic acid.

The mass and flight-time correlation was calculated by using the following equation:

$$m/z = a_{ms} t^2 + b \quad (1)$$

where a is the slope of the calibration curve, t the flight time and b the intercept. The mass axis was calibrated by running different liquid samples with the aerosol mass spectrometer. The samples were applied from a microsyringe directly to the sampling surface, and masses of the fragments were calculated according to their flight times.

The quantitativity was studied with liquid DHB as model substance. The concentration was varied between 2 ppb and 100 ppb, and the sample amount was kept constant at 1 μl. DHB was chosen for the test because it is easily ionized and its spectrum is easily interpreted.

Aerosol measurements

After calibration, the system was tested with selected aerosol samples. Aerosol particle of sucrose (30 nm) and DHB (19 nm) were pro-

duced with the atomizer. Sucrose was dissolved in purified water and DHB in methanol (for the test setup *see* Fig. 1). During the measurements, the valve from the atomizer to the charger was open and the air inlet valve closed. The CPC counted the particles after the DMA, before and after deposition on the collection surface (inlet for the CPC was altered). The particles were also counted during the collection allowing calculation of the collection efficiency and the particle mass. During the sucrose tests the DMA sheath flow was 10 LPM and the aerosol flow 1 LPM. In the DHB tests, the sheath flow was kept at 10 LPM and the aerosol flow was increased to 2 LPM. The collection voltage at the collection surface was +2 kV.

The same system setup was used for qualitative study of ambient aerosol. During the measurements, the valve from the atomizer to the charger was closed. The sampling was done on 28 January 2008 at 10:00 at the Kumpula campus (University of Helsinki, 5 km from the Helsinki city centre). The particle size in the DMA was set to 22 nm. The DMA sheath flow was 10 l min^{-1} and the aerosol flow 2 l min^{-1}. The collection voltage at the collection surface was +2 kV.

Results and discussion

Aerosol time-of-flight mass spectrometer

The aerosol time-of-flight mass spectrometer was constructed to obtain chemical information on ultrafine aerosol particles in near real-time and on site. The operation of the instrument critically depends on the sampling valve, which allows the collection of ultrafine aerosol particles, and the soft laser desorption/ionization which produces good sensitivity. Fragmentation of the compounds is kept at the minimum allowing easier interpretation of the spectra than in the electron ionization. According to Planck's law, the energy of one photon at the wavelength of 193 nm is 6.4 eV. Thus ionization of most organic molecules requires two or three photons.

The pulse-laser system works well with the time-of-flight mass spectrometer since the TOF application requires either a pulsed ionization or pulsed lens voltage system. A linear TOF system design was used. A portable, linear TOF-system is relatively easy to construct, since the only size-limiting factor in the TOF applications is the length of the flight tube; the other parts are already relatively small. We chose 36 cm for the length of the flight tube in order to obtain a resolution of one mass unit. One mass unit resolution was considered satisfactory because our chemical compounds differ by more than 1 mass unit.

The delay between the lasers is important when optimal particle concentration for the MS analysis is required. The delay was determined empirically, and the optimum was found to be about 60 μs. However, it is uncertain what really happens during that 60 μs. Because the energy in one pulse of the desorption laser is in the range of the plasma formation (~10^9 W cm^{-2}; Ready 1971), probably some pseudo-plasma is formed. Since the desorption itself produces ions, basically every desorption and ionization event produces two different spectra, which can be distinguished with a long delay employed. No effort was made to interpret very complex desorption spectra. The low repeatability in the desorption spectrum also indicated some sort of plasma formation in the system. Despite the plasma formation, the desorption and ionization together produce meaningful results that can be followed and used for studies on different chemical compounds.

The ion acceleration system was the most challenging part of the construction. The system exploits two-step ion acceleration. The preliminary ion trajectories were simulated with the Simion 7.0 program, and later acceleration lens voltages were adjusted to their optimal values on the basis of with experimental measurements. The MCP detector was employed because it offers fast time response and is small in size. The system was designed to maintain high vacuum up to 10^{-8} torr. All construction materials used in the vacuum chamber were suitable for high vacuum: i.e., stainless steel, aluminium, Viton, PTFE and polyacetal.

Performance of the sampling valve

Visual inspection confirmed that the sample collection was localized to the sampling surface. A white tissue wetted with methanol turned blue

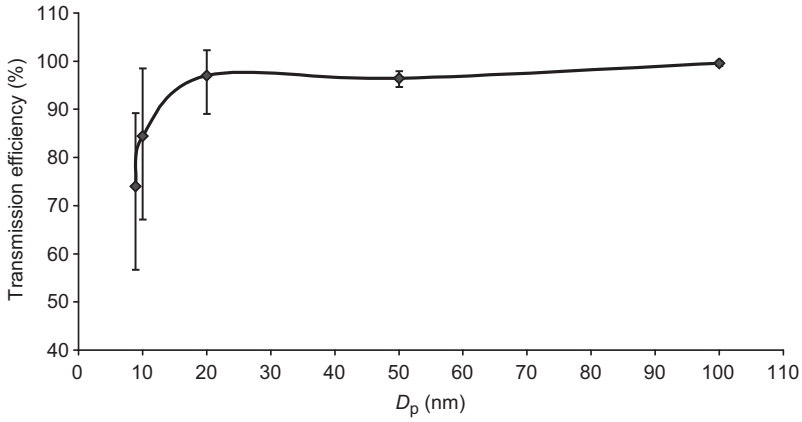

Fig. 3. Transmission efficiency of the valve with the collection voltage turned off. Particles are generated from a sucrose solution with the atomizer. Results are two-minute averages from the CPC, and error bars indicate minimum and maximum values. The aerosol flow rate was 1 l min^{-1}.

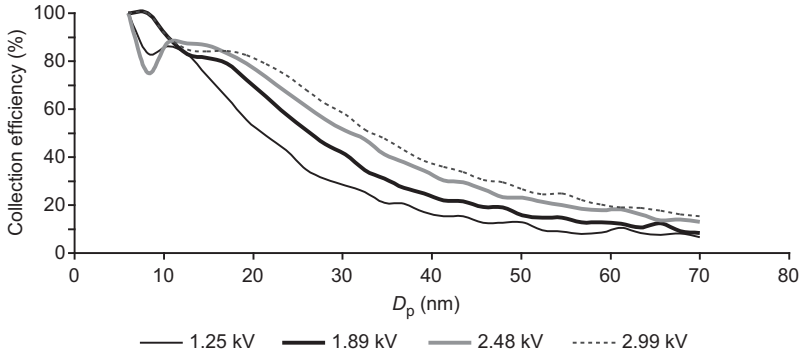

Fig. 4. Collection efficiency of the sampling valve as a function of the particle size for different sample collection voltages.

only when used to clean the collection surface. The study was repeated several times with the same results.

The valve transmission efficiency as a function of particle size was calculated (Fig. 3). As expected, when the particle size was greater than 20 nm, losses were very small. With particle sizes smaller than 20 nm, more particles were lost and errors increased. Even though the system worked in a complex flow environment, the losses in the valve (up to a certain limit) were in practice not important, and the majority of 10-nm particles were collected.

The aerosol flow rate influenced the results. At higher flow rates, the flow close to the collection surface was probably turbulent, causing particle losses in the system. Even though the losses for 10-nm particles were ca. 15%, the collection efficiency was frequently over 85%. Some fraction of the particles were lost in the outlet after the collection surface. If the losses occur because of the turbulent flow close to the collection surface, more particles will be collected with the collection voltage on (*see* Fig. 3).

We calculated collection efficiencies of the sampling valve as a function of the particle size for different voltages. As seen in Fig. 4, they increase with the voltage because of the increased electrostatic force attracting particles towards the surface. The collection efficiency was better for smaller than for larger particles because their electrical mobility is higher. Because of uncertainties in the CPC counting of small particles, 100% collection for 6-nm particles is not realistic. However, the trend is evident.

The scanning electron microscope confirmed that DHB was efficiently desorbed from the stainless steel sampling surface with a single IR laser pulse. After one laser shot, only traces of DHB molecules remained on the sample surface. Note that this test is dependent on the laser power, the sample surface material and its thickness and shape, and also on the sample. This test was done with stainless steel as the sampling surface, but we now use platinum as the sampling surface. Successful desorption (and

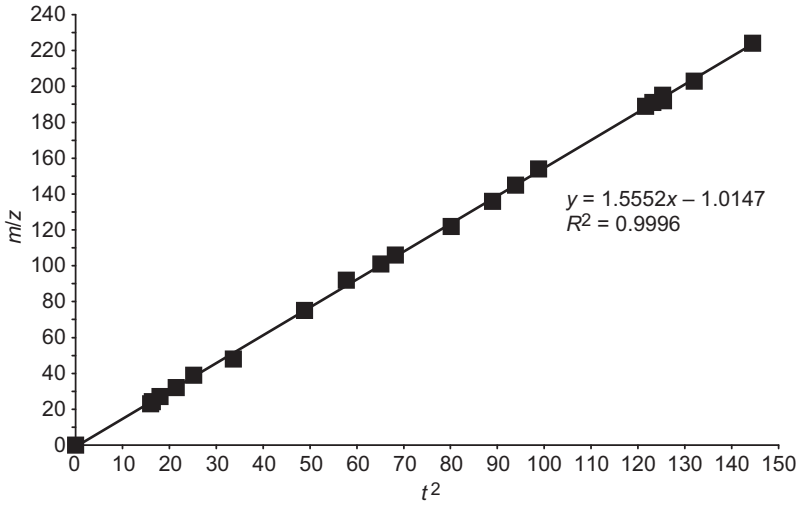

Fig. 5. Calibration curve of the mass axis.

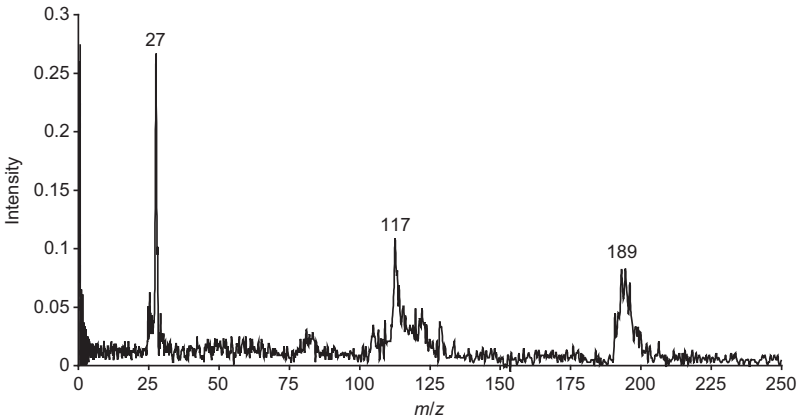

Fig. 6. Mass spectrum of 1 μl of 20 ppm ACCA solution used for calibration of the mass axis.

especially the cleaning of the sampling surface) requires that the size of the sample spot be close to that of the laser beam. Otherwise there is a risk of contamination from the previous sample.

Calibration of the mass axis

The MS calibration curve (Fig. 5) correlates well with the experimental data ($R^2 = 0.9996$), and the data fits well with the theory. There were small variations present in the calibration curve, which were probably caused by variation in the ionization laser firing and unstable energy from pulse to pulse. Also, the pulse jitter in the ionization laser can affect the system.

Three major peaks can be identified in the ACCA spectrum (*see* Fig 6). The peak at *m*/*z* 27 is attributable to aluminium, the peak at *m*/*z* 117 might be due to M^+-$C_2H_2NO_2$ and the peak at *m*/*z* 189 is the molecular ion. Often some aluminium can be seen in the spectra, and occasionally some sodium and potassium are present. Platinum appears when the desorption laser energy is very high. Aluminium is released from the ionization chamber when the ionization laser hits it.

Peaks in the DHB spectrum (Fig. 7) are large. The collection time for DHB was only 6 minutes. The particle concentration at the CPC was about 250 cm^{-3} and the collection efficiency was 97%, which gave a mass of ca. 11 pg at the valve collection surface. There is no peak for aluminium, but there is a large peak for potassium. Potassium is more often present in aerosol samples than in liquid samples. Other peaks from DHB are at *m*/*z* 80, 108, 136, where 136 is the main peak and corresponds to M^+-H_2O. The M^+ ion of DHB is only seen at higher concentrations.

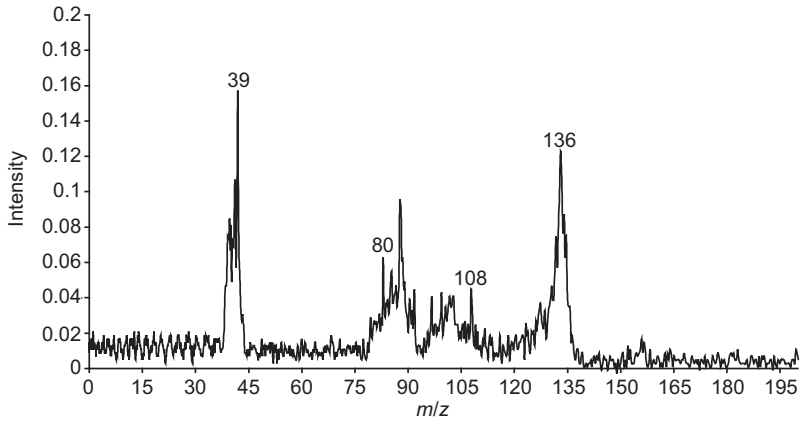

Fig. 7. Mass spectrum of 19 nm DHB aerosol particles.

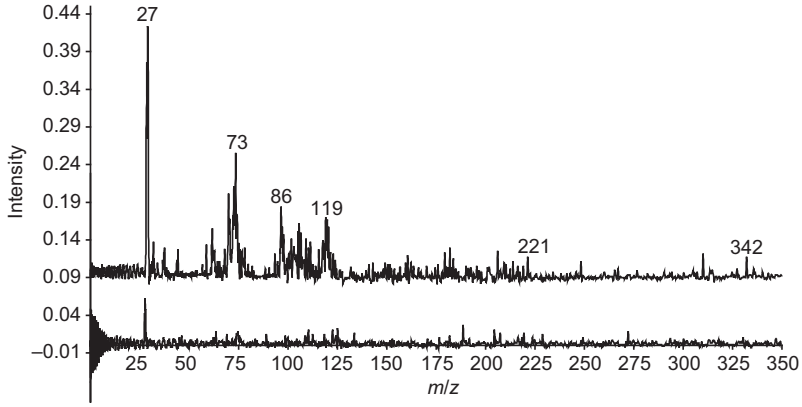

Fig. 8. Mass spectrum of 30 nm sucrose aerosol particles.

For DHB, the linear range of our system was about 10–100 ppb. After 100 ppb the baseline became unstable. Note that this test showed a response only for this particular compound, and the response may differ with the compound due to the selective nature of the ionization laser. DHB was easily detected with our system because of the good absorbance at 193 nm.

Aerosol measurements

The system was tested with aerosol samples (Fig. 8). The collection time for the sucrose was 23 minutes and the particle concentration at the CPC during the measurements was about 750 cm^{-3}. The collection efficiency was 96%, which gave a mass of ca. 0.23 ng at the valve collection surface. The spectrum is a bit messy, but some major fragments can be identified. Also, the similarity with the general EI spectrum is apparent. The spectrum of a blank sample run before the aerosol collection is shown in Fig. 8 under the test spectrum. The sole peak in the blank sample spectrum is due to aluminum.

The aerosol mass spectrometer was capable of detecting compounds at sub-picogram concentrations present in aerosol particles from ambient air (Fig. 9). The collection time was 31 minutes and the collection efficiency was 95%. The particle concentration at the CPC was about 12 cm^{-3} for that particle size. This concentration gave a mass of ca. 4 pg at the valve collection surface.

Identifying individual compounds from a mixed spectrum can be difficult, especially when the resolution is relatively low and the background is noisy. The largest mass peaks are at around *m*/*z* 27, 73 and 119. The peak at *m*/*z* 27 is attributable to aluminum from the ionization chamber, and that at *m*/*z* 73 probably refers to alkane chains. Alkanes would be expected in an environment like this. The other peaks in the spectrum are difficult to identify. Many more

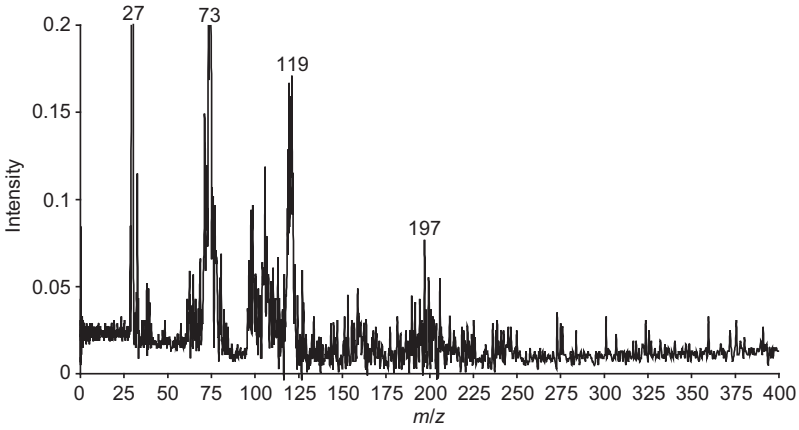

Fig. 9. Mass spectrum of 22 nm ambient aerosol sample.

measurements would be required to determine with certainty the chemical composition of the atmosphere for a particular particle size at a particular moment. High mass resolution and MS-MS analysis would be most valuable in resolving complex spectra like the one in Fig. 9.

Conclusions

An aerosol time-of-flight mass spectrometer incorporating laser desorption and ionization combined with particle collection on a metal surface was constructed. All parts of the system were tested and their performance as a whole was confirmed. The aerosol MS was sensitive for the analysis of ultrafine aerosol particles with low mass resolution. The small size of the instrument makes it well suited for field use. Less vacuum pumping capacity is needed because there is no gas flow to the MS system. Aerosol mass spectrometry was successfully applied to the study of selected organic compounds in aerosol particles. Mass spectra could easily be obtained for ambient air particles as small as 22 nm. Further research is needed to reveal the full potential of the system and to obtain better spectra. The potential of MS-MS for the system also needs to be investigated. Currently, we are seeking to integrate the size-selective collection with the valve through control of the collection voltage and the rate of aerosol flow onto the surface of the valve.

Acknowledgements: The funding by the Academy of Finland Centre of Excellence program (project no. 1118615) is acknowledged. Financial support was also provided by the Finnish Funding Agency for Technology and Innovation, Tekes. Pekka Tarkiainen, Mikael Ehn, Matti Jussila, Erkki Siivola, Kari Kuuspalo, Markku Rasilainen, Timo Kivi, Heikki Lihavainen, Alexey Adamov and Pasi Aalto are thanked for technical help. Special thanks are addressed to Irmeli Mustonen at Nordic Aluminium for surface treatments in the ionization chamber and to Seppo Levänen at Metso Automation for the sampling valve ball.

References

Allan J.D., Alfarra M.R., Bower K.N., Coe H., Jayne J.T., Worsnop D.R., Aalto P.P., Kulmala M., Hyötyläinen T., Cavalli F. & Laaksonen A. 2006. Size and composition measurements of background aerosol and new particle growth in a Finnish forest during QUEST 2 using Aerodyne Aerosol Mass Spectrometer. *Atmos. Chem. Phys.* 6: 315–327.

Allen T.M., Bezabeh D.Z., Smith C.H., McCauley E.M., Jones A.D., Chang D.P.Y., Kennedy I.M. & Kelly P.B. 1996. Speciation of arsenic oxides using laser desorption/ionization time-of-flight mass spectrometry. *Anal. Chem.* 68: 4052–4059.

Anttila P., Hyötyläinen T., Heikkilä A., Jussila M., Finell J., Kulmala M. & Riekkola M.-L. 2005. Determination of organic acids in aerosol particles from a coniferous forest by liquid chromatography-mass spectrometry. *J. Sep. Sci.* 28: 337–346.

Emmenegger C., Kalberer M., Samburova V. & Zenobi R. 2004. Analysis of size-segregated aerosol-bound polycyclic aromatic hydrocarbons with high time resolution using two-step laser mass spectrometry. *Analyst* 129: 416–420.

Ge Z., Wexler A.S. & Johnston M.V. 1998. Laser desorption/ionization of single ultrafine multicomponent aerosols. *Environ. Sci. Technol.* 32: 3218–3223.

Gross H.J. 2004. *Mass spectrometry; a textbook*. Springer, Germany.

Gu L.H., Baldocchi D.D., Wofsy S.C., Munger J.W., Michal-

sky J.J., Urbanski S.P. & Boden T.A. 2003. Response of a deciduous forest to the Mount Pinatubo eruption: Enhanced photosynthesis. *Science* 299: 2035–2038.

Hartonen K., Kuuspalo K., Lihavainen H., Aalto P., Rasilainen M., Riekkola M.-L., Kulmala M. & Viisanen Y. 2006. *Sampling device for introducing of samples into analysis system*. US Patent Application 11/438689.

Haefliger O.P. & Zenobi R. 1998. Laser mass spectrometric analysis of polycyclic aromatic hydrocarbons with wide wavelength range laser multiphoton ionization spectroscopy. *Anal. Chem.* 70: 2660–2665.

Heard D.E. 2006. *Analytical techniques for atmospheric measurement*. Blackwell, UK.

Johnston M.V. 2000. Sampling and analysis of individual particles by aerosol mass spectrometry. *J. Mass Spectrom.* 35: 585–595.

Kaelberer M., Morrical B.D., Sax M. & Zenobi R. 2002. Picogram quantitation of polycyclic aromatic hydrocarbons adsorbed on aerosol particles by two-step laser mass spectrometry. *Anal. Chem.* 74: 3492–3497.

Kulmala M., Vehkamäki H., Petäjä T., Dal Maso M., Boy M., Lauri A., Kerminen V.-M., Birmili W. & McMurry P.H. 2004. Formation and growth rates of ultrafine atmospheric particles: a review of observations. *J. Aerosol. Sci.* 35: 143–176.

Liu P., Ziemann P.J. Kittelson D.B. & McMurry P.H. 1995. Generating particle beams of controlled dimensions and divergence. I. Theory of particle motion in aerodynamic lenses and nozzle expansions. *Aerosol Sci. Technol.* 22: 293–313.

Liu P., Ziemann P.J. Kittelson D.B. & McMurry P.H. 1995. Generating particle beams of controlled dimensions and divergence. II. Experimental evaluation of particle motion in aerodynamic lenses and nozzle expansions. *Aerosol Sci. Technol.* 22: 314–324.

Lohmann U. & Feichter J. 2005. Global indirect aerosol effects. *Atmos. Chem. Phys.* 5: 715–737.

Mallina R.V., Wexler A.S., Rhoads K.P. & Johnston M.V. 2000. High speed particle beam generation: a dynamic focusing mechanism for selecting ultrafine particles. *Aerosol Sci. Technol.* 33: 87–104.

McMurry P.H. 2000. A review of atmospheric aerosol measurements. *Atmos. Environ.* 34: 1959–1999.

Morrical B.D., Fergenson D.P. & Prather K.A. 1998. Coupling two-step laser desorption ionization with aerosol time-of-flight mass spectrometry for the analysis of individual organic particles. *J. Am. Soc. Mass. Spectrom.* 9: 1068–1073.

Nash D.G., Baer T. & Johnston M.V. 2006. Aerosol mass spectrometry: An introductory review. *Int. J. Mass Spectrom.* 258: 2–12.

Ready J.F. 1971. *Effects of high-power laser radiation*. Academic press, USA.

Reinnig M.-C., Müller L., Warnke J. & Hoffmann T. 2008. Characterization of selected organic compounds classes in secondary organic aerosol from biogenic VOCs by HPLC-MSn. *Anal. Bioanal. Chem.* 391: 171–182.

Shimmo M., Saarnio K., Aalto P., Hartonen K., Hyötyläinen T., Kulmala M. & Riekkola M.-L. 2004. Particle size distribution and gas-particle partition of polyaromatic hydrocarbons in Helsinki urban area. *J. Atmos. Chem.* 47: 223–241.

Smith J.N., Moore K.F., McMurry P.H. & Eisele F.L. 2004a. Atmospheric measurements of sub-20 nm diameter particle chemical composition by thermal desorption chemical ionization mass spectrometry. *Aerosol Sci. Technol.* 38: 100–110.

Smith J.N., Moore K.F., Eisele F.L., Voisin D., Ghimire A.K., Sakurai H. & McMurry P.H. 2004b. Chemical composition of atmospheric nanoparticles during nucleation events in Atlanta. *J. Geophys. Res.* 110: 1–13.

Stieb D.M, Judek S. & Burnett R.T. 2002. Meta-analysis of time-series studies of air pollution and mortality: Effects of gases and particles and their influence of cause of death, age and season. *J. Air Manage. Assoc.* 52: 470–484.

Trimborn A., Hinz K.-P. & Spengler B. 2000. Online analysis of atmospheric particles with a transportable laser mass spectrometer. *Aerosol Sci. Technol.* 33: 191–201.

Voisin D., Smith J.N., Sakurai H., McMurry P.H. & Eisele F.L. 2003. Thermal desorption chemical ionization mass spectrometer for ultrafine particle chemical composition. *Aerosol Sci. Technol.* 37: 471–475.

Wang X. & McMurry P.H. 2006. An experimental study of nanoparticle focusing with aerodynamic lenses. *Int. J. of Mass Spectrom.* 258: 30–36.

Wang S.Y., Zordan C.A. & Johnston M.V. 2006. Chemical characterization of individual, airborne sub-10 nm particles and molecules. *Anal. Chem.* 78: 1750–1754.

Warnke J., Bandur R. & Hoffmann T. 2006. Capillary-HPLC-ESI-MS/MS method for the determination of acidic products from the oxidation of monoterpenes in atmospheric aerosol samples. *Anal. Bioanal. Chem.* 385: 34–45.

Öktem B., Tolocka M.P. & Johnston M.V. 2004. On-line analysis of organic components in fine and ultrafine particles by photoionization aerosol mass spectrometry. *Anal. Chem.* 76: 253–261.